Using stereo SAR and InSAR by combining the COSMO-SkyMed and the TanDEM-X mission satellites for estimation of absolute height

K. ELDHUSET and D. J. WEYDAHL
Norwegian Defence Research Establishment (FFI)
Land and Air Systems Division
PO Box 25, NO-2027 Kjeller, Norway
e-mail: knut.eldhuset@ffi.no; dan-johan.weydahl@ffi.no

Abstract. The objective of this work is to estimate absolute heights in SAR interferograms. Since heights in interferograms are relative, we use stereo SAR with several satellites to achieve absolute height references of natural or manmade reflectors. We study the performance of stereo height estimation and geographic positioning using each of the satellites TerraSAR-X (TSX) and COSMO-SkyMed (CSK) as well as combination of both satellites. Corner reflectors positioned by GPS are used as reference. The accuracy obtained with corner reflectors may be the best we can expect using SAR for height estimation and geolocation. The location errors in this study were less than 0.6 m for TSX alone, 1.5 m for CSK alone or combined with TSX. By combining TSX and CSK, stereo SAR is applied to estimate absolute heights in bistatic interferograms generated from TSX and TanDEM-X (TDX). This method seems to yield absolute height accuracy in interferograms better than 1-2 meters.

1. Introduction

In the last few years a new era in space borne SAR remote sensing has been opened due to the advent of four COSMO-SkyMed (CSK-1,2,3,4) satellites, TerraSAR-X (TSX) and TanDEM-X (TDX). TSX was launched on 15 June 2007 (Breit *et al.* 2010) with resolution around 1 m. The COSMO-SkyMed constellation satellites were launched in the period from 8 June 2007 to 7 November 2010 and secured fast response and almost the same resolution as TSX (Covello *et al*. 2010). TDX was launched on 21 June 2010 (Rodriguez-Cassola *et al.* 2012). All satellites can be used for stereo height estimation or interferometry (InSAR) . The main purpose of the TanDEM-X mission using TDX and TSX is to generate a global digital elevation model (DEM). The absolute height error is mostly below 10 m before DEM calibration (Bachmann *et al.* 2012). In (Gonzalez *et al.* 2010) they use accurate height references provided by the Ice, Cloud and land Elevation Satellite (ICESat) for calibration of the DEM. The height accuracy of these ground control points (GCPs) can be as good as 0.5 m, however, they are historical data. When using ICESat data for calibration, it is possible to achieve absolute height accuracy around 1-2 meters (Huber *et al.* 2012). It was demonstrated in (Eldhuset *et al.* 2011) that stereo SAR can be used to yield absolute height accuracy of a few decimetres for well-defined point targets using the TSX satellite alone. Here we propose an alternative way to generate height references by using stereo image pairs from one satellite or combining different satellites, e.g. TSX and CSK-1. By using one of the CSK satellites, the time difference between the TSX/TDX interferogram and the stereo SAR image pair can be minimized. If we have an interferogram generated from TSX and TDX in close tandem formation, we can use TSX and one of the CSK satellites to estimate

Dette er en postprint-versjon / This is a postprint version.
DOI til publisert versjon / DOI to published version: 10.1080/01431161.2013.843808

reference heights. We call this technique Stereo Interferometric SAR or abbreviated as StInSAR .

In Chapter 2 we describe the SAR data set and the corner reflectors used. A very brief review of the stereo height estimation and geolocation algorithms is given in Chapter 3. A refinement of geolocation accuracy is performed by estimation of residual Doppler using the SAR image products. In Chapter 4 we apply these algorithms using TSX and CSK data for assessment of the accuracy of the method using corner reflectors which have been located with GPS. The idea is to use natural or man made reflectors as stereo points and a short assessment of this method is provided. We use corner reflectors for this analysis because we cannot expect that the accuracy using other reflectors exeeds the accuracy using corner reflectors. In Chapter 5 we give an example where we select a man made reflector as a stereo point and estimate its absolute height. This point is then used as a reference to achieve the absolute heights in an interferogram. If two strong points are selected for stereo matching, the algorithm gives a number how good the match is. The physical nature need not be known. The important thing is that the target looks as a strong point with a homogeneous region around it in both images .

2. Data set and corner reflectors

2.1 Data set

We have several high-resolution TerraSAR-X spotlight and COSMO-SkyMed spotlight images available from the test sites at Zeebrugge in Belgium (June 2011). The images were all processed to single look complex (SSC) products. The TerraSAR-X images are processed by DLR and distributed by Astrium GEO-Information Services, Germany, while the COSMO-SkyMed data are processed and distributed by e-GEOS, Italy. The TerraSAR-X and COSMO-SkyMed SAR data acquired over Zeebrugge in Belgium were collected in a demonstration project carried out jointly by Infoterra and e-Geos, and the NATO SET-145 research group. We received the CoSSC TandDEM-X data from the Norwegian Forest and Landscape Institute in an AO-project. The images used in this work are listed in table 1.

2.2 Radar corner reflectors

Several trihedral triangular (or square) corner reflectors were deployed within the area of the acquired TerraSAR-X and COSMO-SkyMed scenes over Zeebrugge in Belgium. The corner reflectors were deployed by the NATO SET-145 group under responsibility of Fraunhofer IOSB in Germany and the Royal Military Academy in Belgium. Our radar corners are constructed in a special way: each of the corner objects consist of four trihedral or square corners that are mounted together back-to-back in order to give a strong backscatter from a variety of azimuth angles (figure 1). The positions and heights of the 4 corner reflectors are given in table 2. The corner reflectors on the harbour (#2 and #3) are shown in a TerraSAR-X image in the left image of figure 2 . The right image in figure 2 shows a Google image. The other reflectors are also located in the harbour region. The orthometric heights are all between 5 and 6 m and the maximum azimuth and range distances are 634 and 916 pixels, respectively. Our corner reflectors were oriented in more or less East-West

directions. This may give an azimuth angle offset up to as much as 20 degrees for the ascending/descending polar orbiting SAR sensors at these latitudes. However, with this simple configuration, we could use the same corner reflector in both ascending and descending satellite pass without the need for turning the corner reflectors in between the different SAR acquisitions.

Also, the reflectors were deployed with one of the trihedral plates in the horizontal plane (i.e. no tilt). This will normally produce a maximum backscatter for radar incidence angles at 55 degrees. However, our SAR acquisitions had incidence angles ranging from 27 to 49 degrees (table 1). This will introduce offset angles from 6 to 28 degrees in elevation. Now, despite the non-optimal azimuth and elevation angles, the corner reflectors still produced strong and well defined point scatterers in the processed SAR images as shown in figure 2. These points were thus used as reference targets. The centre position of the radar corner reflectors were measured in June 2011 with a differential GPS system.

3. Stereo height estimation and geolocation

FFI (Forsvarets Forskningsinstitutt or Norwegian Defence Research Establishment) has developed a high-precision SAR pixel position algorithm (FFI SAR pixel position algorithm) for satellite SAR images. The algorithm uses a two-step approach to solve a set of non-linear equations. Based on a selected pixel position within the satellite SAR image (range and azimuth pixel number), the algorithm calculates the geodetic latitude and longitude position of that pixel using an ellipsoid such as the WGS84. The maximum intensity of the corner reflectors are found by two dimensional interpolation using splines. Then the stereo height is estimated followed by the FFI SAR pixel position algorithm which does not use the attitude data provided in the SAR products. Input parameters in the FFI SAR pixel position algorithm is the zero-Doppler time of a given pixel, the slant range given in the product header and an ellipsoid where the stereo height is added to the WGS84 ellipsoid. The output are absolute height, latitude and longitude in the ITRF 2008 (International Terrestrial Reference Frame) for the data in table 1. These parameters are then compared with the same parameters determined by GPS in the WGS84 system (table 2). We refer to (Eldhuset *et al.* 2011) for the details of the algorithm above.

In (Schubert *et al.* 2010) in the second last paragraph of Section VI it is mentioned that they found an average azimuth offset in the TSX products. In (Eldhuset *et al.* 2011) we discovered that this azimuth offset was not the same in all scenes. Since an azimuth time offset can be associated with a Doppler different from zero in a zero Doppler product we developed an algorithm to estimate the residual Doppler as described in Section IV.D in (Eldhuset et al. 2011). For a pixel with given azimuth and range we calculated the (X,Y,Z) in a rotating earth system from the geographic latitude and longitude and reference height provided in the TSX product (<GEOREF.xml> file) or the CSK product and used the satellite state vector (in a rotating earth system) for the same azimuth time as given for the pixel. For the TSX or TDX satellites the calibration azimuth offset can be used prior to estimation of residual Doppler, however, the final position is not changed because another residual Doppler is estimated if it is not used. Quite many grid points with (latitude, longitude, height) are given in the <GEOREF.xml> file in the TSX and TDX products. In the CSK products only the corner points and centre point of the scene are available. The residual Doppler varies from scene to scene. For the three TSX scenes used here the residual Doppler was less than 1 Hz (0.85 Hz corresponds to 1 m azimuth offset),

Dette er en postprint-versjon / This is a postprint version.
DOI til publisert versjon / DOI to published version: 10.1080/01431161.2013.843808

however, the variation could also be up to 0.5 Hz over the scene in azimuth direction. In range direction the values were almost constant. One example is shown in table 3 for TSX. The maximum value found in the CSK images was 0.5 Hz and a variation of 0.4 Hz over one scene in azimuth direction. These numbers indicate that some products are not exactly zero Doppler processed. Corrections for this residual Doppler allowed us to obtain a few decimetres accuracy in azimuth direction.

4. Results from stereo height estimation and geolocation

Tables 4,5,6,7 show stereo height estimation followed by geolocation using spotlight data. We note that the input height for geolocation is the stereo estimated value and **not** the height provided by the GPS system. In (Schubert *et al.* 2010 and 2011) they did their GPS measurements of the corner reflectors within the CHTRF95 reference frame. This reference frame drifts relative to the ITRF system with 2-3 cm /year (due to continental drift) . The total drift since 1989 is nearly 50 cm. The GPS positions in table 2 are given in the WGS84 and in our work in (Eldhuset et al. 2011) the positions of the corner reflectors were given in WGS84 and in the ITRF reference frames (ITRF 2005 and ITRF 2008). The state vectors in this work are given in the ITRF 2008 reference frame. The difference of the latest versions of WGS84 and the ITRF are only few centimeters (Schubert et al. 2010, Cong *et al.* 2012). Therefore continental drift will hardly be detected in our data. Tropospheric and ionospheric delays are given in the TSX and TDX products and we use these numbers to correct the slant range. In the CSK products these delays are not available, however, the slant range seems to be compensated.

This analysis will show the accuracies of the latitude, longitude and height (ΔLat, ΔLon, ΔH) using the SAR system alone (no external DEMs or GPS measurements). We only use the GPS measurements of the corner reflectors as a comparison. Tables 4 and 5 show the accuracies of longitude, latitude and height achieved with two different stereo combinations with and without using the residual Doppler estimates. Without using the residual Doppler the latitude error is around 0.9 m in table 4 and around 1 m in table 5. Using the residual Doppler estimate improves the accuracy and yield latitude errors less than 2 cm in table 4 and less than 15 cm in table 5. The longitude and height errors change only 10-15 cm using the residual Doppler. The longitude errors in table 5 are better than 20 cm and in Table 4 they are less than 60 cm. The magnitude of the height errors and longitude errors differ a few decimeters. A wrong stereo estimate of the height will appear as a longitude error mainly.

Tables 6 and 7 show results for both opposite and same side stereo height estimation. From table 6 we see that for COSMO-SkyMed alone the same parameters as in tables 4 and 5 are all less than 1m for the parallaxes which are greater than 22.1 m. The mean latitude error in table 6 is 0.3 m and the standard deviation is 0.46 m. The mean longitude error is 1.2 m with standard deviation 0.33 m. Some of the combinations are the same but with the satellites exchanged. We see that some of the parallax values are the same for these combinations: 22.1 m, 132.4 m and 133.8 m. The height values for these cases are also roughly the same, however, latitudes and longitudes are more different. The mean height error is -0.17 m with standard deviation 0.34 m. Latitude errors are mainly along the azimuth direction and longitude errors in range direction. Hence, table 6 tells us that for the CSK satellites that the mean error in azimuth direction is just a few decimetres from zero. We also remember from Chapter 3 that the residual Doppler was less than 0.5 Hz for the CSK satellites. This means that the zero-Doppler product of COSMO-SkyMed may cause azimuth

Dette er en postprint-versjon / This is a postprint version.
DOI til publisert versjon / DOI to published version: 10.1080/01431161.2013.843808

position errors around 0.5 m. The mean longitude error in range is 1.2 m which may be caused by two effects: atmospheric variations which have not been sufficiently compensated in the product combined with the stereo height errors which cause position errors in range direction. From table 7 we see that for parallax greater than 40 m the latitude, longitude and height errors are less than 1.5 m. For parallax values less than 9-10 m the height errors are as large as 6 m. The table tells us that the parallax should not be too small. We therefore omitted the combinations with parallax 9.1 m, 10.5 m and 10.8 m for mean and standard deviation estimations. The estimated results based on this approach produced a mean latitude error of 0.07 m with standard deviation 0.17 m, mean longitude error 0.00 m and standard deviation 0.98 m. The mean height error is -0.15 m and the standard deviation 0.90 m. We see that for the cross-sensor combinations (table 7) the standard deviations are larger both for longitude and height compared to same sensor combinations (table 6). The latitude accuracies are better in table 7 than in table 6.

It is of course an advantage to have corner reflectors deployed for estimation of reference points. However, if no corner reflectors are deployed it may still be possible to find distinct common points for the stereo estimation either on buildings or natural reflectors. We have checked several such points in both CSK and TSX strip map and spot light mode images. For example, as shown in (Eldhuset *et al*. 2011) the height of roof windows were estimated with a few decimeter accuracy using stereo SAR. If the parallax is sufficiently large and the points are well suited for stereo estimation, our results so far show that the height error may be 1- 2 m or better depending on the type of reflector.

5. Stereo interferometric SAR (StInSAR) absolute height estimation

Figure 3 shows a bistatic TanDEM-X interferogram processed with FFI software from the TSX and TDX CoSSC (Coregistered Single-look Slant-range Complex) products acquired in strip map mode over the Lardal municipality in South Norway. No GCPs were used for generation of the interferogram. The mean coherence over the scene is 0.8. The Lardal valley extends from north to south in the right part of the image. The phase of the interferogram has been converted to altitude (meters) using the computed height of ambiguity (which varies over the scene). A test site is selected within the small white frame in figure 3 around the dam in the lake called Mykle. Figure 4 shows a zoom in the same region where two small areas H1 and H2 are indicated. H1 is close to the lake. We selected the frame H2 such that the mean height within the frame achieved maximum. In this way the maximum corresponds to the terrain peak in the map shown in figure 5. The relative height between the small frames H1 and H2 is estimated from the interferogram to be 126.0 m. Figure 5 shows a map with the dam and a peak in the lower left corner which is 549 m above sea level. Then we selected a common strong point in the two stereo images shown in figure 6. The dam is enclosed by a circle in each of the images.We assume that this strong backscatter comes from somewhere in the dam hatch. The stereo height is estimated to 423.3 m and we see from the map that the 425 m contour line is in the same level as the top of the dam. The selected frame H1 is near the lake and close to the 425 m contour line in the map south of the dam. If we take the sum of the stereo height and the relative height in the interferogram we get: 423.3 m+126.0 m=549.3 m. This is accidentally the same height as the height of the peak in the map (rounded off to meters) which indicates that the center of reflection from the dam hatch (say 1.7 m below the top of the dam) and from the ground in frame H1 in figure 5 are at same

height. An aerial photo of the region where the terrain peak is located shows sparse forest, hence, the radar height is probably close to the ground.

We checked several cases in this interferogram with distinct stereo points and found 1-2 m difference from the map. We compared the relative height differences extracted from the interferogram, with a topographic map in the same region. In the Lardal valley we took some agricultural flat areas where we could average many pixels. The difference from the map was less than 1.5 m for two sites approximately 30 km apart as the crow flies. This means that one stereo estimated absolute height should suffice to achieve better than 2 m absolute height error of a DEM generated from a bistatic TanDEM-X interferogram.

We should note that in figure 6 the angles of incidence of TSX and CSK are 42° and 29°, respectively. Hence, the SAR backscatter may change considerably since the difference of the angles is 13°. Accidentally, we had this stereo pair available, however, it should be possible to find pairs with a smaller difference between the angles of incidence. We can see from table 7 that using TSX D 30° and CSK4 D 27° yields a height error of 4.3 m which is quite large. In this case the difference of the angles of incidence is only 3° which is too small for achieving good height accuracy. A good choice of difference in the radar incidence angles should therefore be investigated before making acquisitions in an operational monitoring system.

6. Conclusions

We have used software developed at FFI for pixel location, stereo height estimation and InSAR processing to estimate absolute heights in TanDEM-X bistatic interferograms. We used deployed corner reflectors and estimated latitude, longitude and stereo height using TSX and CSK separately. In addition we combined TSX and CSK. The best height accuracies were obtained with TSX alone (better than 0.6 m). For CSK alone or combined with TSX, the errors were estimated to less than 1.3 m for sufficiently large parallax. We have also found that the height accuracy for distinct stereo points found in nature or from buildings may be 1-2 m depending on the properties of the scattering surface or object. The references below tell that historic ICEsat altimetry data are being used for calibration (absolute height estimation) of TanDEM-X DEMs. We have shown here that the CSK satellites combined with the TSX satellite in the TanDEM-X mission can be used to estimate absolute height references using the stereo SAR technique. This method may be a supplement for calibration of the TanDEM-X DEMs with all data acquired very close in time, only limited by an appropriate stereo pair from TSX and one of the four CSK satellites.

Acknowledgment

This work was supported by the Norwegian Defence Research Establishment (NDRE). We thank Svein Solberg at the Norwegian Forest and Landscape Institute for providing the CoSSC TanDEM-X data (AO-project XTI_VEGE0315). We like to thank Karsten Schulz at IOSB Fraunhofer in Germany for lending out several of their radar corner reflectors that were used in the Zeebrugge campaign but also Dirk Borghys at Royal Military Academy (RMA) in Belgium for organizing the deployment and the GPS measurements of the radar corner reflectors. GPS measurements were carried out by the team of Alain Muls at the RMA. We also thank Astrium GEO-Information Services and e-GEOS for making satellite SAR images

available over Zeebrugge during the common demo project that was carried out between these organizations and the NATO SET-145 working group.

References

BACHMANN, M., GONZALEZ, J.H., KRIEGER, G., SCHWERDT, M., ANTONY, J.W., and DEZAN, F., 2012, Calibration of the Bistatic TanDEM-X Interferometer. Proceedings of the European Conference on Synthetic Aperture Radar (EUSAR 2012), Nürnberg, Germany, 23-26 April 2012.

BREIT, H., FRITZ, T., BALSS, U., LACHAISE , M., NIEDERMAIER , A., and VONAVKA, M., 2010, TerraSAR-X SAR Processing and Products. *IEEE Transactions on Geoscience and Remote Sensing*, **48**, 727-740.

CONG, X., BALSS, U., EINEDER, M., FRITZ, T., 2012 ,Imaging Geodesy-Centimeter-Level Ranging Accuracy With TerraSAR-X. *IEEE Transactions on Geoscience and Remote Sensing*, 9, 948-952.

COVELLO, F., BATTAZZA, F., COLETTA, A., LOPINTO, E., FIORENTINO, C., PIETRANERA, L., VALENTINI, G., and ZOFFOLI, S., 2010, COSMO-Skimmed an existing opportunity for observing the Earth. *Journal of Geodynamics*, **49**, 171-181.

ELDHUSET, K., and WEYDAHL, D.J., 2011, Geolocation and Stereo Height Estimation Using TerraSAR-X Spotlight Image Data. IEEE Transactions on Geoscience and Remote Sensing, 49, 3574-3581.

GONZALES, J.H., BACHMANN, M., KRIEGER, G., and FIEDLER, H., 2010, Development of the TanDEM-X Calibration Concept: Analysis of Systematic Errors. *IEEE Transactions on Geoscience and Remote Sensing*, 48, 716-726.

HUBER, M., GRUBER, A., WESSEL, B., BREUNIG, M., and WENDLEDER, A., 2012,Validation of tie-point concepts by the DEM adjustment approach of TanDEM-X. Proceedings of the European Conference on Synthetic Aperture Radar (EUSAR 2012), Nürnberg, Germany, 23-26 April 2012.

RODRIGUEZ-CASSOLA, M., PRATS , P., SCHULZE, D., TOUS-RAMON, N., STEINBRECHER, U., MAROTTI, L., NANNINI, M., YOUNIS, M.,LOPEZ-DEKKER, P., ZINK, M., REIGBER, A., KRIEGER, G., and MOREIRA, A., 2012, First Bistatic Spaceborne SAR Experiment With TanDEM-X. *IEEE Transactions on Geoscience and Remote Sensing*, **9**, 33-37.

SCHUBERT, A., JEHLE, M., SMALL, D., and MEIER, E., 2010, Influence of Atmospheric Path Delay on the Absolute Geolocation Accuracy of TerraSAR-X High_resolution Products. *IEEE Transactions on Geoscience and Remote Sensing*, **48**, 751-758.

SCHUBERT, A., JEHLE, M., SMALL, D. and MEIER. E., 2011, Mitigation of Atmospheric and Solid Earth Movements in a TerraSAR-X Time-Series. *Journal of Geodesy*, (Online).

Figure 1 Two of the radar corner reflectors that were deployed in Zeebrugge harbour by Fraunhofer IOSB in (left) and Royal Military Academy (right). The size of the reflectors are around 0.5 m.

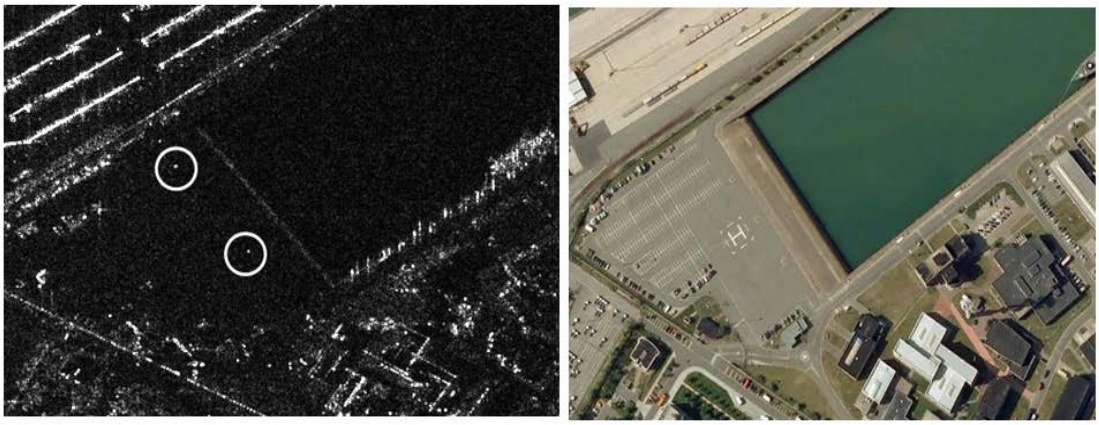

Figure 2 Left: TSX image (26 June 2011) with incidence angle around 42°. The radar reflectors in figure 1 are enclosed with two circles. TerraSAR-X data were distributed by Astrium GEO-Information Services, © DLR 2011. Right: Google image.

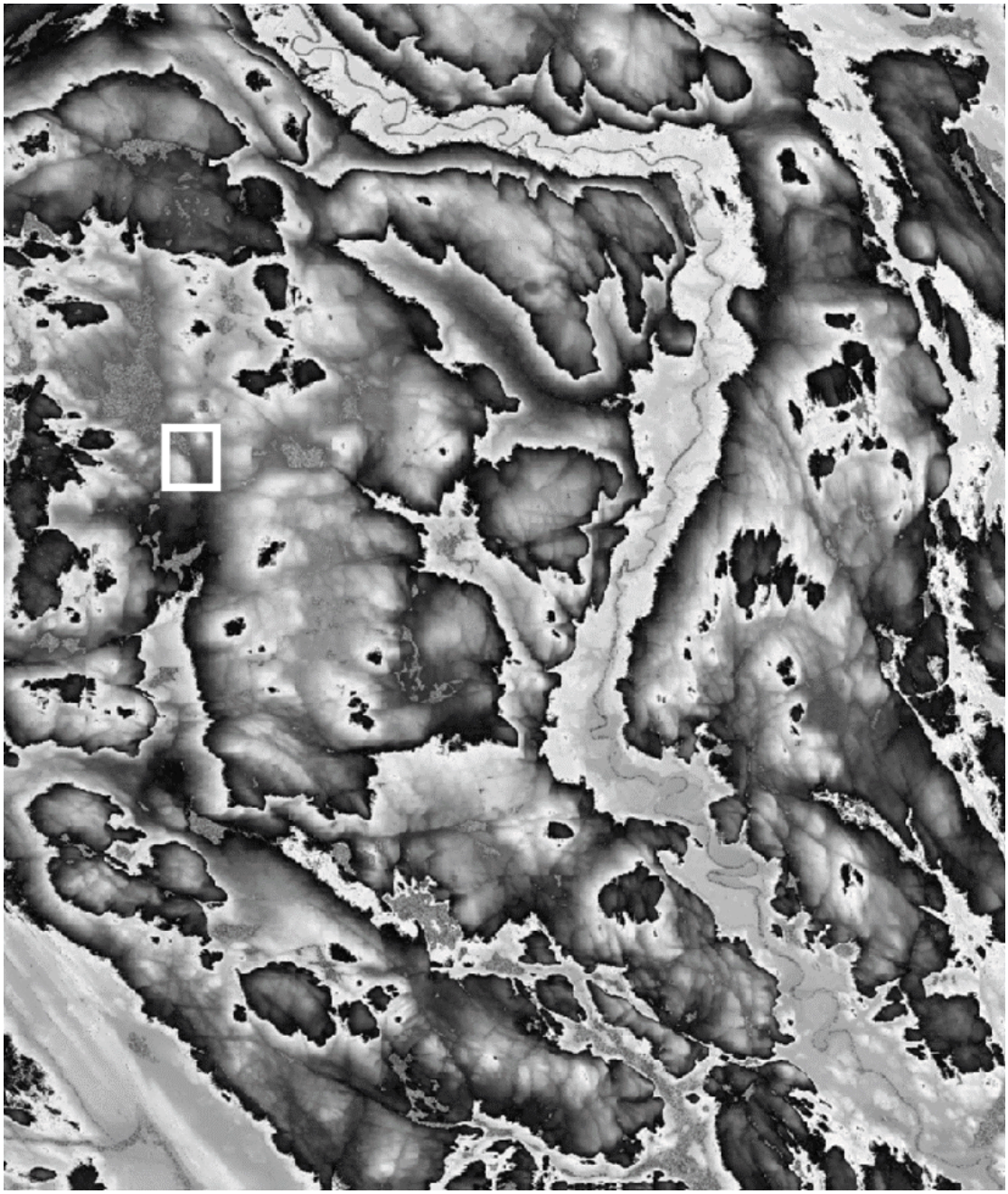

Figure 3 TanDEM-X bistatic slant range interferogram strip map mode (horizontal range, vertical azimuth) processed at FFI from the CoSSC product. The scene center is at latitude 59.3547° and longitude 9.8543° and averaged 5 azimuth x 7 range pixels. Start time is 2011-09-01 05:40:54.7974. The image covers 44.1 km in azimuth and 25.5 km in range. The image in the white frame is zoomed in figure 4.

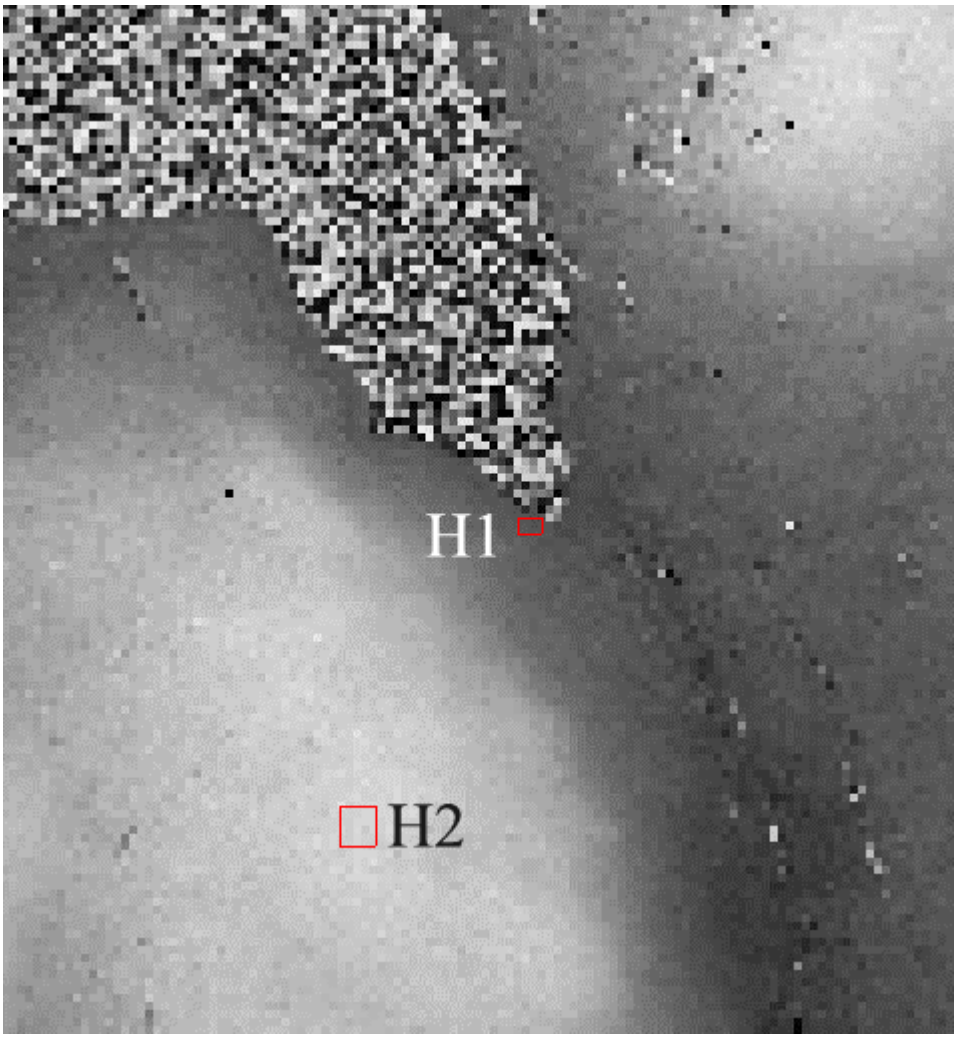

Figure 4 TanDEM-X bistatic interferogram (zoomed) in the area around the dam in the lake Mykle shown in the white frame in figure 3.

DOI til publisert versjon / DOI to published version: 10.1080/01431161.2013.843808

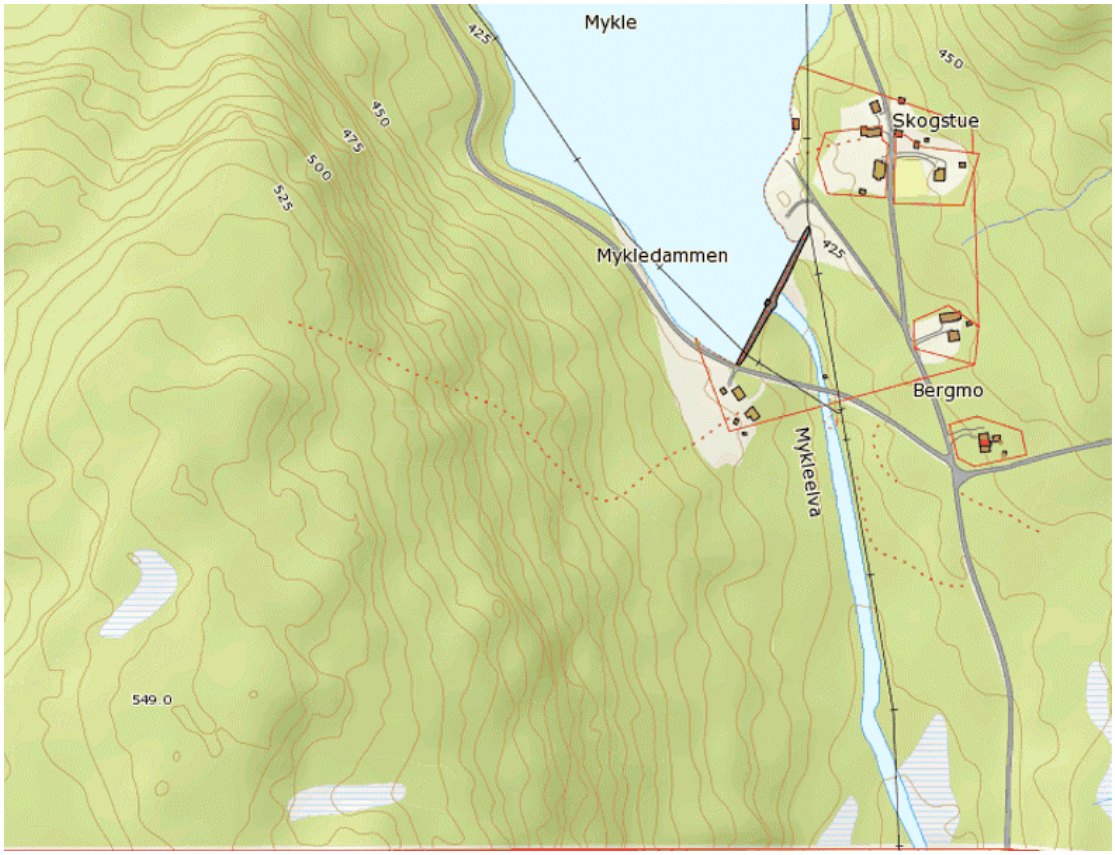

Figure 5 A map (www.norgeskart.no) corresponding to the area shown in the interferogram in figure 4. The latitude at the dam is 59.4157° and the longitude is 9.6996 °.

Dette er en postprint-versjon / This is a postprint version.
DOI til publisert versjon / DOI to published version: 10.1080/01431161.2013.843808

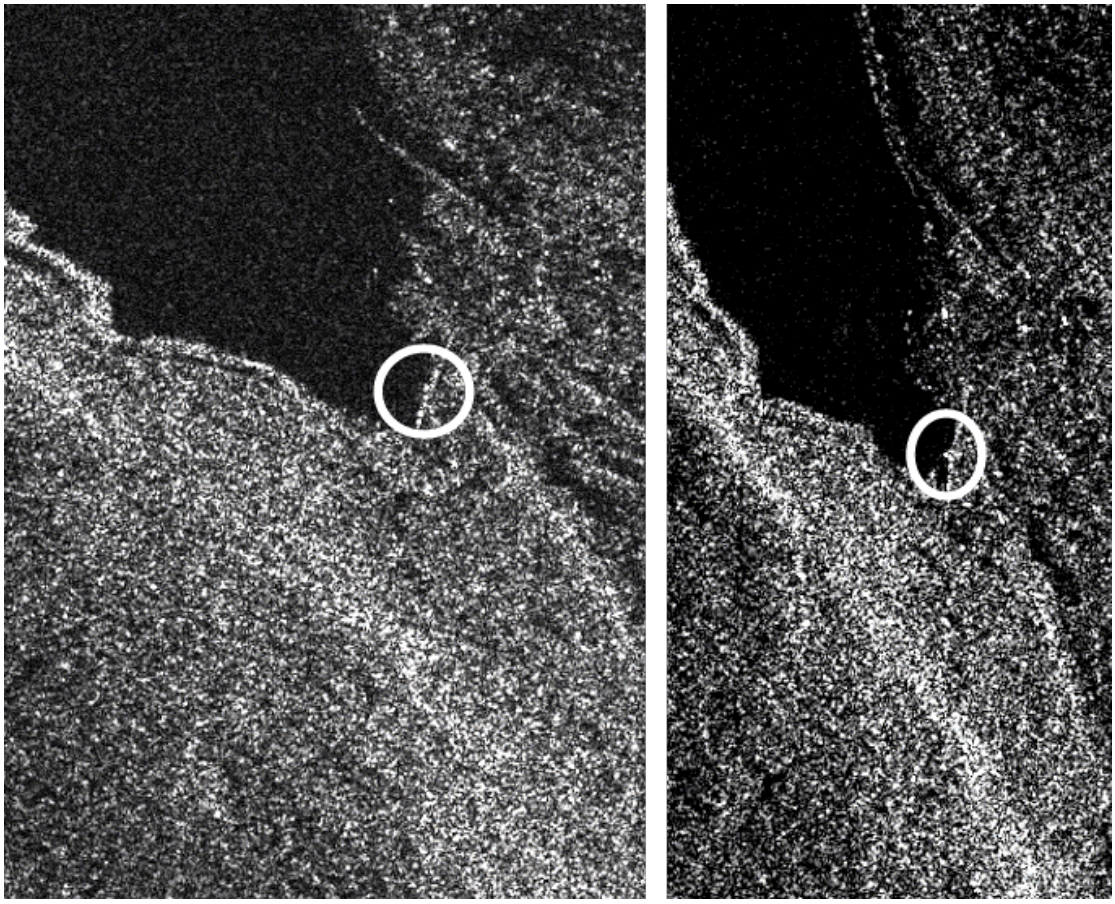

Figure 6 Stereo pair of images (not anaglyph) around the dam in the lake Mykle, TSX (1 Sept 2011) to the left and CSK3 (11 July 2009) to the right. The stereo points are located at the center of each of the white circles. The incidence angle of TSX is around 42° and for CSK 29° . The ground pixel spacing is 1.34 m for TSX and 2.16 m for CSK. TerraSAR-X data were distributed by Astrium GEO-Information Services, © DLR 2011. CSK data were distributed by e-GEOS, © COSMO-SkyMed™ Product -ASI 2009, processed under license from ASI – Agenzia Spaziale Italiana.

DOI til publisert versjon / DOI to published version: 10.1080/01431161.2013.843808

Table 1 The different satellite images used in this study. The first 8 images are used for stereo SAR and images #9 and #10 are a Tandem-X bistatic image pair used for processing of the interferogram in figure 3. Image #11 is combined with image #9 for StInSAR. Image #1 is denoted as TSX D 42° (15 June) in subsequent text and the other images likewise.

Image	**Satellite**	**Mode**	**Descending/Ascending**	**Incidence angle(°)**	**Date**
#1	TSX	SpotLight	D	42	15 June 2011
#2	TSX	SpotLight	D	30	20 June 2011
#3	TSX	SpotLight	D	42	26 June 2011
#4	CSK 1	SpotLight	A	37	20 June 2011
#5	CSK 2	SpotLight	D	27	15 June 2011
#6	CSK 3	SpotLight	A	49	19 June 2011
#7	CSK 3	SpotLight	D	27	16 June 2011
#8	CSK 4	SpotLight	D	27	19 June 2011
#9	TSX	StripMap	D	42	1 September 2011
#10	TDX	StripMap	D	42	1 September 2011
#11	CSK 2	StripMap	D	29	10 July 2009

Table 2 GPS latitude and longitude of the four corner reflectors given in the WGS84 reference frame. Azimuth and range in Image #1 in table 1 are provided and the orthometric GPS height of each reflector.

Corner reflector	Latitude Deg.-min.-sec.	Longitude Deg.-min.-sec.	Azimuth in Image #1	Range in Image #1	Orthometric height(m)
#1	51-20-9.1954	3-11-53.5842	4442	5022	5.52
#2	51-20-12.3773	3-12-24.4032	4217	4175	5.29
#3	51-20-14.1502	3-12-27.3393	4144	4106	5.63
#4	51-20-25.3021	3-12-12.3587	3808	4614	5.50

DOI til publisert versjon / DOI to published version: 10.1080/01431161.2013.843808

Table 3 Residual Doppler estimates for TSX scene #2 in Table 1 for 9 grid points in the <GEOREF.xml> file. The size of the scene is 6302 x 11101 pixels.

	azimuth=1	azimuth=3438	azimuth=6302
range=1	0.539 Hz	0.700 Hz	0.957 Hz
range=4996	0.537 Hz	0.697 Hz	0.953 Hz
range=11101	0.534 Hz	0.694 Hz	0.948 Hz

Table 4 Results from TerraSAR-X geolocation and height estimations using stereo SAR scenes alone. The parallax is 30.7 m. Deployed radar corner reflectors in Zeebrugge were used to estimate stereo positions. 'D' means descending pass followed by the angle of incidence.

TerraSAR-X stereo TSX D 30° (20June) and TSX D 42° (26 June)	**Δ Lat [m]**	**Δ Lon [m]**	**Δ H [m]**
Without residual Doppler			
Reflector no.1	0.88	0.48	-0.32
Reflector no.2	0.86	0.21	-0.21
Reflector no.3	0.86	0.33	-0.53
Reflector no.4	0.87	0.54	-0.36
With residual Doppler			
Reflector no.1	0.01	0.51	-0.44
Reflector no.2	-0.02	0.24	-0.32
Reflector no.3	-0.02	0.36	-0.64
Reflector no.4	-0.01	0.61	-0.50

Table 5 Results from TerraSAR-X geolocation and height estimations using stereo SAR scenes alone. The parallax is 30.8 m.

TerraSAR-X stereo TSX D 42° (15 June) and TSX D 30° (20 June)	**Δ Lat [m]**	**Δ Lon [m]**	**Δ H [m]**
Without residual Doppler			
Reflector no.1	0.94	0.11	-0.12
Reflector no.2	1.10	0.26	-0.21
Reflector no.3	1.15	-0.14	-0.21
Reflector no.4	0.97	0.24	-0.19
With residual Doppler			
Reflector no.1	-0.15	0.06	-0.24
Reflector no.2	0.00	0.21	-0.33
Reflector no.3	0.06	-0.19	-0.33
Reflector no.4	-0.12	0.20	-0.44

Dette er en postprint-versjon / This is a postprint version.
DOI til publisert versjon / DOI to published version: 10.1080/01431161.2013.843808

Table 6 Results from COSMO-SkyMed geolocation and height estimations using stereo SAR scenes alone. Reflector no 2 is used. 'D' means descending pass and 'A' ascending pass followed by the angle of incidence. Deployed radar corner reflectors in Zeebrugge were used to estimate stereo positions.

COSMO-SkyMed stereo combination from Zeebrugge harbour	**Δ Lat [m]**	**Δ Lon [m]**	**Δ H [m]**	**Parallax [m]**
CSK3 A 49° & CSK1 A 37°	-0.23	1.97	0.33	22.1
CSK1 A 37° & CSK3 A 49°	0.85	1.56	0.33	22.1
CSK3 A 49° & CSK2 D 27°	-0.38	0.85	-0.75	132.3
CSK3 A 49° & CSK3 D 27°	-0.28	1.54	-0.28	134.1
CSK3 A 49° & CSK4 D 27°	-0.30	1.44	-0.32	133.8
CSK1 A 37° & CSK3 D 27°	0.76	1.00	0.10	155.4
CSK1 A 37° & CSK4 D 27°	0.77	1.04	-0.09	155.1
CSK1 A 37° & CSK2 D 27°	0.73	0.91	0.02	153.7
CSK2 D 27° & CSK3 A 49°	0.53	0.85	-0.69	132.4
CSK2 D 27° & CSK1 A 37°	0.62	0.96	-0.48	153.8
CSK4 D 27° & CSK3 A 49°	0.30	1.30	-0.20	133.8
CSK4 D 27° & CSK1 A 37°	0.28	1.09	0.05	155.4

Table 7 Results from cross-sensor stereo combinations of TerraSAR-X and COSMO-SkyMed. Reflector no. 2 is used. 'D' means descending pass and 'A' ascending pass followed by the angle of incidence.

TSX and CSK stereo combination from Zeebrugge harbour	**ΔLat [m]**	**ΔLon [m]**	**ΔH [m]**	**Parallax [m]**
TSX D 42° (26 June) & CSK4 D 27°	0.24	-1.02	0.86	41.2
TSX D 42° (26 June) & CSK3 D 27°	0.31	-1.43	1.25	41.5
TSX D 42° (15 June) & CSK3 D 27°	0.31	-1.52	1.31	41.5
TSX D 42° (26 June) & CSK2 D 27°	-0.09	0.91	-0.95	39.7
TSX D 42° (15 June) & CSK2 D 27°	-0.10	0.82	-0.90	39.7
TSX D 30° (15 June) & CSK4 D 27°	1.52	-7.41	4.30	10.5
TSX D 30° (20 June) & CSK3 D 27°	2.08	-10.2	5.98	10.8
TSX D 30° (20 June) & CSK2 D 27°	-1.04	5.32	-3.4	9.1
TSX D 42° (15 June) & CSK4 D 27°	0.24	-1.10	0.91	41.2
TSX D 42° (26 June) & CSK1 A 37°	0.00	0.46	-0.53	114.8
TSX D 30° (20 June) & CSK3 A 49°	-0.18	1.04	-0.82	123.3
TSX D 42° (26 June) & CSK3 A 49°	-0.09	0.94	-0.98	93.2
TSX D 42° (15 June) & CSK1 A 37°	-0.02	-0.44	-0.54	114.8
TSX D 42° (15 June) & CSK3 A 49°	-0.11	0.91	-0.98	93.2
TSX D 30° (20 June) & CSK1 A 37°	-0.07	0.49	-0.48	144.7

DOI til publisert versjon / DOI to published version: 10.1080/01431161.2013.843808